

A dissipated energy maximization approach to elastic-perfectly plastic analysis of planar frames

Dedicated to the late Prof. J. A. König for his valuable research on exactness of mathematical programming approaches in plasticity

M. R. MAHINI¹⁾, H. MOHARRAMI¹⁾, G. COCCHETTI²⁾

¹⁾*Department of Structural Engineering
Tarbiat Modares University
14115-397 Tehran, Iran
e-mails: mahini@modares.ac.ir; hamid@modares.ac.ir*

²⁾*Department of Structural Engineering
Technical University (Politecnico) of Milan
Piazza L. da Vinci
32-20133 Milan, Italy
e-mail: cocchett@stru.polimi.it*

THE OPTIMIZATION APPROACHES, known as powerful tools in nonlinear analysis of structures, are considered in this paper for further development. Adopting linear kinematics, proportional loading, lumped plasticity, piecewise-linear yield loci, perfect plasticity and associated flow rule as the basic assumptions, the nonlinear analysis of a framed structure is formulated in the form of a mathematical programming problem. Dissipated energy is considered as the objective function and is maximized using the conventional simplex method with special provisions to obtain exact structural responses. The proposed algorithm is validated and outlined using several numerical examples taken from the literature.

Key words: frame nonlinear analysis, perfect plasticity, mathematical programming, piecewise-linear models, lumped plasticity.

Copyright © 2013 by IPPT PAN

1. Introduction

ANALYSIS OF ELASTO-PLASTIC STRUCTURES is nowadays a primary design requirement for practicing engineers. Accordingly, it has become a frequently addressed and well-known engineering problem in the literature (see, e.g., [1–3]).

Linear programming (LP) has long been recognized as a suitable tool for limit state analysis of structures [4]. To this end, by assuming lumped plasticity, i.e., localizing plasticity in some prescribed sections and considering rigid-plastic behavior for the structure, the limit load of the frame is sought from an LP problem.

In this sense, depending on the way the problem is formulated and the approach is followed, i.e., lower bound or upper bound theorems, the problem will appear in the form of maximization or minimization of linear programming [5, 6]. MAIER proposed the use of quadratic programming (QP) in structural mechanics, and by considering the complementarity conditions as the objective function, formulated elasto-plastic structural problems in the form of QP problems [7, 8]. Later on, adopting piecewise-linear (PWL) elasto-plasticity with interacting yield planes, the proposed method was extended to matrix structural analysis [9]. To improve the efficiency of the solution procedure, QP was replaced by the linear complementarity problem (LCP) [10], and the restricted basis linear programming (RBLP) [11]. Application of mathematical programming (MP) in elasto-plastic analysis has been the subject of interest to several researchers. For example, virtual distortion method, which was primarily proposed by HOLNICKI-SZULC and GIERLINSKI [12] to impose the effects of prestressing into the structural elements and reanalysis of structures, has been implemented in nonlinear analysis of the structures in combination with mathematical programming by GAWECKI and KUCZMA [13]. In this approach, at each level of loading, the effect of plasticity in a specific location of the frame is imposed through some virtual internal deformations. Also employing MP in nonlinear analysis has been improved and extended to more general cases such as shakedown and nonlinear dynamic analyses [14, 15].

COCCHETTI and MAIER [16] implemented the aforementioned approach in analysis of frames with softening plastic hinges. They proposed two procedures, namely step-by-step method, and stepwise-holonomic/fully-holonomic method. In the step-by-step method, in each step the load is increased up to development of a plastic hinge in the structure after which the next load step starts. This approach provides the exact solution to the problem, but it is required to rearrange vectors and matrices by separating the problem variables into active and non-active sets by solving an LCP subproblem. Clearly, this fact becomes computationally disadvantageous when numerous yield modes can be activated in many critical sections simultaneously and/or in small intervals. It is worth noting that the word “exact” means that this approach does not let any approximations enter the final results, except those coming from the accepted simplifying assumptions. In addition, stability of the solvers of this kind is guaranteed, even in the presence of softening. Exactness and unconditional stability are the most important aspects of this method in spite of the disadvantages addressed before.

In order to reduce the number of sub-step amplitudes, one may disregard the path dependency of the solution within each load step. In this case, the stepwise or fully holonomic solutions with arbitrary load step sizes are used. Using this approach, probable unloading during some steps or, generally saying, leaving any yield plane could not be captured and this feature turns out to be a potential source

of error, typical in holonomic approaches. In both proposed solution schemes, the load multiplier is considered as the objective function to be maximized, subject to the yield and complementarity conditions. Such an approach will encounter problems in the case of softening frames and when the decreasing branch of the response initiates. This is addressed in [16] as elastic unloading and it is emphasized that the subproblem has to be re-solved for negative load increment if no solution is found for the positive load increment. Following the unique equilibrium path without a need for successive LCP solutions and ruling out problems raised due to negative load increments, were the main motivations of this research although the softening behavior is not addressed in the present study.

Recently, another approach has been presented by TANGARAMVONG and TIN-LOI to deal with the structures governed by piecewise-linear softening models [17]. This method has a holonomic character and is similar to that discussed in [16], but employs a penalty approach to solve the nonlinear optimization problem. In this approach, decision on initial value and updating schedule of the penalty parameter, which enforce the complementarity conditions, has to be taken carefully to prevent numerical instabilities. Besides this and similarly to each holonomic approach, to reduce errors due to ignoring path dependency, the load steps have to be considered very small.

In all approaches based on mathematical programming, the final solution at the end of load step is of interest and plastic deformations are computed according to the final location of stress state on the yield surface. This fact does not result in any divergence from the exact solution in step-by-step solution scheme, but the holonomic approaches are sensitive to this assumption and accuracy of the results depends on the step sizes.

In this paper, by assuming linear kinematics and lumped plasticity, nonlinear analysis of a proportionally loaded frame is formulated in an MP form. To this end, piecewise-linear yield surfaces and associated flow rule are adopted to construct the required elastic-perfectly-plastic hinge constitutive model. Conventional simplex method with special provisions is employed to propose a solution strategy. In the proposed algorithm, two distinct features of step-by-step method, namely “exactness” and “stability” are preserved. In addition, the linear complementarity problem (LCP), that has to be solved at each step, is replaced by a maximum dissipation criterion. In all tested examples, the results show that the outcome of this proposed method is equivalent to LCP, but they are obtained in a more efficient way.

2. Formulation

At the beginning of any nonlinear analysis, a conventional linear elastic analysis is performed to determine the linear elastic responses of the structure, i.e.,

internal forces \mathbf{p}^0 , internal deformations \mathbf{u}^0 and nodal displacements \mathbf{U}^0 for the given load level:

$$(2.1) \quad \mathbf{U}^0 = \mathbf{K}^{-1}\mathbf{R}, \quad \mathbf{u}^0 = \mathbf{A}\mathbf{K}^{-1}\mathbf{R}, \quad \mathbf{p}^0 = \mathbf{k}\mathbf{A}\mathbf{K}^{-1}\mathbf{R}.$$

In the above formulas, \mathbf{R} is external load vector, \mathbf{K} is initial stiffness matrix of structure, \mathbf{k} is elements block-diagonal stiffness matrix, and \mathbf{A} stands for compatibility matrix.

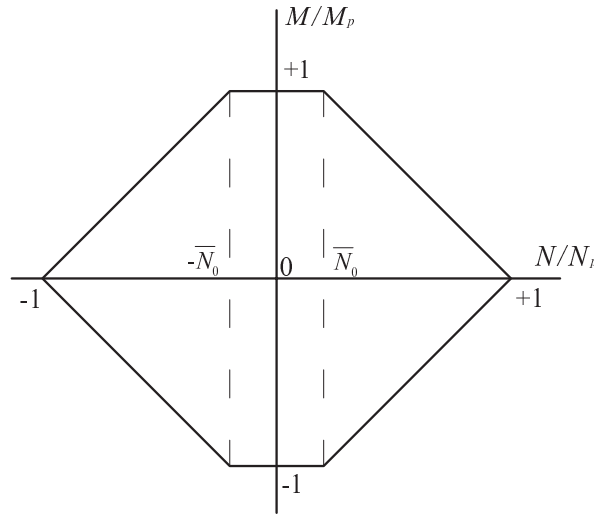


FIG. 1. A typical piecewise-linear plastic hinge model.

In the second step, internal forces have to be verified to see whether they satisfy yield conditions or not. To this end, similar to that shown in Fig. 1, it is conventional to adopt some piecewise-linear constitutive model [18, 19]. It is obvious that the full plastic axial capacity of frame members is rarely achievable in real cases due to the member instabilities, i.e., column buckling, but herein geometric nonlinearities are not accounted for. Considering the internal force vector \mathbf{p}_i containing the internal axial force N^i and the bending moment M^i at section i :

$$(2.2) \quad \mathbf{p}_i = \begin{Bmatrix} N^i \\ M^i \end{Bmatrix},$$

the yield conditions at this section can be stated as follows:

$$(2.3) \quad \mathbf{\Phi}_i^T \mathbf{p}_i \leq \{1\}.$$

The yield matrix Φ_i in Eq. (2.3) corresponds to the governing constitutive model of the frame section, which for the six-line yield locus ($m = 6$) shown in Fig. 1, is of the form:

$$(2.4) \quad \Phi_i = \begin{bmatrix} \frac{1}{N_p^i} & 0 & \frac{-1}{N_p^i} & \frac{-1}{N_p^i} & 0 & \frac{1}{N_p^i} \\ \frac{1 - \bar{N}_0^i}{M_p^i} & \frac{1}{M_p^i} & \frac{1 - \bar{N}_0^i}{M_p^i} & \frac{\bar{N}_0^i - 1}{M_p^i} & \frac{-1}{M_p^i} & \frac{\bar{N}_0^i - 1}{M_p^i} \end{bmatrix}.$$

The parameter \bar{N}_0^i , refers to the ordinate of the corners in the yield locus and is defined as follows:

$$(2.5) \quad \bar{N}_0^i = \frac{N_0^i}{N_p^i}.$$

And, as shown in Fig. 1, N_0^i is the axial force corresponding to the yield surface corner in section i . The plastic deformations u_i^p , in a typical section, can be related to the section's plastic multipliers x_i using the yield matrix Φ_i , by the so-called associated flow rule as follows:

$$(2.6) \quad u_i^p = \left\{ \begin{matrix} \Delta_p^i \\ \theta_p^i \end{matrix} \right\} = \Phi_i x_i,$$

where $x_i = \{x_i^1 \ x_i^2 \ \dots \ x_i^m\}^T$ is a vector containing plastic multipliers corresponding to each yield plane at section i .

The presented piecewise-linear elasto-plastic formulas at the local level can be easily extended to the global level by assembling local yield matrices and plastic multiplier vectors. Considering n as the whole number of critical sections, the global plastic multipliers vector \mathbf{x} and yield matrix Φ are defined as follows. Note that \mathbf{x} is composed of n vectors of dimension $m \times 1$

$$(2.7) \quad \mathbf{x} = \left\{ \begin{matrix} x_1 \\ x_2 \\ \vdots \\ x_n \end{matrix} \right\}, \quad \Phi = \begin{bmatrix} \Phi_1 & & & \mathbf{0} \\ & \Phi_2 & & \\ & & \ddots & \\ \mathbf{0} & & & \Phi_n \end{bmatrix}.$$

Also in order to describe the coupling effects of plasticity among sections, some influence matrices \mathbf{p}^v (for internal forces) and \mathbf{U}^v (for nodal displacements) have to be developed. Each column of the influence matrices contains linear elastic response of the structure to a unit's internal deformation imposed in the corresponding critical section. It should be noted that such analyses, which have to be done only once at the start, do not require any stiffness matrix assembly

or further inversion to that already done for primary linear elastic analysis. Using influence matrices and plastic deformations (Eq. (2.6)), the residual nodal displacements U^P and residual internal forces p^P are determined as follows:

$$(2.8) \quad p^P = \mathbf{p}^v \Phi_{\mathbf{x}}, \quad U^P = \mathbf{U}^v \Phi_{\mathbf{x}}.$$

Also the additivity rule is assumed to hold for internal forces p , internal deformations u and nodal displacements U as follows:

$$(2.9) \quad p = p^e + p^P, \quad u = u^e + u^P, \quad U = U^e + U^P.$$

Where, those parts denoted by a superscript e are the linear elastic response of the structure under the current external actions level, and are calculated by scaling the primary responses identified by Eq. (2.1). Accordingly, at any load level λ , total responses of the structure are computed using the following formulas:

$$(2.10) \quad p = \lambda p^0 + \mathbf{p}^v \Phi_{\mathbf{x}}, \quad u = \lambda u^0 + \Phi_{\mathbf{x}}, \quad U = \lambda U^0 + \mathbf{U}^v \Phi_{\mathbf{x}}.$$

The yield conditions to be satisfied at all critical sections can be stated as follows:

$$(2.11) \quad Y = \lambda \Phi^T p^0 + \Phi^T \mathbf{p}^v \Phi_{\mathbf{x}} - \{1\} \leq 0.$$

Furthermore the objective function, that in this study is considered to be dissipated power, i.e., plastic work rate, has to be developed. It can be easily verified that the plastic work rate at any loading stage is equal to sum of all active plastic multipliers rates (see Appendix A).

Then, according to the assumed maximum dissipation criterion, an optimization problem can be written for the whole structure (in terms of all yield functions, the increments of plastic multipliers and load multiplier increment) as follows (see Appendix B):

$$(2.12) \quad \begin{cases} \max \{1\}^T \dot{\mathbf{x}} \\ \text{subject to:} \\ Y = \lambda \Phi^T p^0 + \Phi^T \mathbf{p}^v \Phi_{\mathbf{x}} - \{1\} \leq 0, \\ \mathbf{x}^T \mathbf{Y} = 0, \mathbf{x} \geq 0, \bar{\lambda} \geq \lambda \geq 0. \end{cases}$$

In the above problem, $\bar{\lambda}$ is the maximum load level defined by user. To capture any probable collapse it is conventional to add a deflection control constraint of the form $\Delta \leq \bar{\Delta}$ to the problem, in which $\bar{\Delta}$ can be a limit on deflection at any desired node. As it will be discussed in the next section, this MP has to be solved in increments and accordingly at each step the load and plastic multipliers resulted from the previous steps will cause some reduction in the remaining strength capacity of sections and the term $\{1\}$ in yield constraints $Y \leq 0$ will be automatically modified at each step.

3. Solution procedure

In the following, some details are given about the proposed algorithm for solving the MP defined by Eq. (2.12). In the literature, CLP and RBLP are proposed for solving MP problems of this kind, in which the nonlinear complementarity constraints $x^T Y = 0$ are satisfied implicitly during solution. In these solution strategies, simultaneous presence of a plastic multiplier x_i^j (corresponding to the j -th yield plane of the critical section i) and its counterpart slack variable y_i^j in the base vector is prevented. But as stated before, such a restriction is not sufficient to ensure exact solutions. In this study, some extra provisions, namely “*resetting*” and “*refreshing*”, will be proposed to be considered in combination with aforementioned restriction.

Generally speaking, at any loading instant, the plastic multipliers x may be formally classified into three categories: first, those which have zero values and belonging to non-active yield planes (“inactive”); second, those corresponding to active yield planes and will potentially react to further load application (“active”), and third the plastic multipliers with nonzero values which do not change during a load step (“passive”). Third group of plastic multipliers may appear in some critical sections due to local unloading or passing a yield surface corner.

On the other hand and as a consequence of the PWL models for local nonlinear behavior, some *events* may happen during analysis. These *events* are the stress state changes relating to “*leaving yield surface*”, “*transit from one yield surface to adjacent one*” and “*staying on a yield surface corner*”. Obviously if such an *event* does not happen, the response of a frame structure to external actions varying proportionally (or stepwise proportionally) can be computed “exactly” [16, 20]. However, any plasticity *event* that causes a local change in this proportionality, is deemed to be a source of divergence from exact response. To the knowledge of authors, any subproblem that is formed and solved after each load step in a step-by-step solution scheme, is basically an attempt to detect any oncoming *event* and recognize any active plastic multiplier that tends to join the passive plastic multipliers. By eliminating those plastic multipliers in the next MP, the unique equilibrium path of the structure is captured. Mathematically saying, the MP problem (2.12) over a loading interval which is defined between two successive *events*, is no longer nonconvex and even a holonomic approach can return exact solutions on such an interval. Accordingly, in order to cancel probability of any error development and accumulation during solution, the load levels corresponding to the *events* have to be determined and the solution has to be followed in a *refreshed* simplex table after a *resetting*.

Resetting means recording the current load and corresponding values of plastic multipliers and resuming solution by considering the achieved external load level and internal forces as the initial conditions for structure in an updated

mathematical programming. The resetting is simply done by setting to zero the right-hand side of active constraints in the simplex table. It is worth noting that after resetting, the simplex table represents an MP problem corresponding to the latest structure's status, which is identical to what is obtained by modifying (2.12) using the following substitutions:

$$(3.1) \quad \lambda = \hat{\lambda} + \dot{\lambda}, \quad \mathbf{x} = \hat{\mathbf{x}} + \dot{\mathbf{x}},$$

wherein, hatted variables are referred to the latest achieved values for the problem variables and dotted ones are new expected increments.

Refreshed simplex table is referred to the updated form of the simplex table after performing required pivot actions for exiting a plastic multiplier, if unloading is the case. Fortunately this refreshment does not impose any computational effort except three pivotings per each unloading in the simplex table.

To start the solution process, the initial table of linear programming is constructed as shown in Table 1. This table is an expanded matrix representation of the yield and other inequality constraints, which are turned into equalities using some slack variables. In this table, γ and δ are slack variables corresponding to the load multiplier λ and displacement Δ , respectively. Also $\bar{\lambda}$ and $\bar{\Delta}$ are some limits imposed on the load multiplier λ and the monitored displacement Δ , respectively. The superscripts and subscripts specify the yield plane and section numbers, respectively. Since there is one variable x for each yield plane, the matrix of coefficients $\bar{\mathbf{C}}$ is square. This matrix is identified by light gray in Table 1. To solve the problem a set of slack variables y should be added. The matrix $\overline{\bar{\mathbf{C}}}$, which is recognized by dark gray in Table 1, provides a canonical form of the basis matrix for starting the LP solution.

Since each row of the simplex table corresponds to a yield plane, hereafter the variables x and y are addressed with only one subscript which refers to the row number where their corresponding "yield plane constraint" is placed in the simplex table.

The procedure followed for solution of this table is very similar to the RBLP method (which utilizes standard simplex method with some additional provisions for considering complementarity conditions), but herein additional tasks have to be taken to detect any *events* defined above. This procedure is better demonstrated in the flowchart of Fig. 2 and the following descriptions corresponding to each step.

Step 1. To start manipulation, it is noted that at the beginning, all y variables are present in the set of basic variables (BV); therefore, as a result of complementarity constraints none of x variables can enter the BV. Evidently, without letting the load multiplier λ to assume a value, no plastic hinge can form; therefore, the first variable that enters the BV is the load

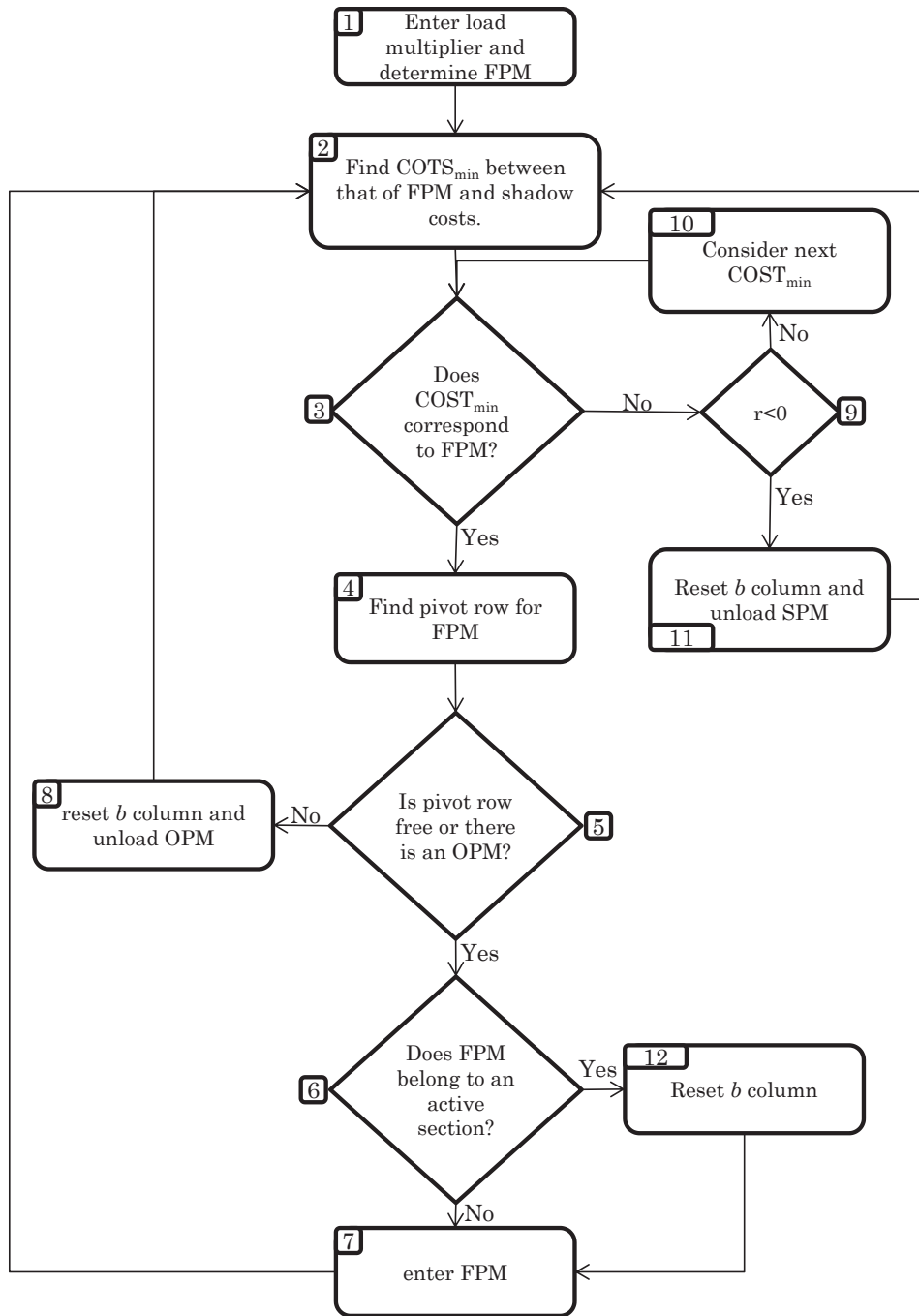


FIG. 2. Solution flowchart.

multiplier λ . At this time, according to the simplex rules, a pivot row with minimum positive $b_j/\overline{C}(j, i)$ ratio has to be determined for the exiting variable. Then, the pivoting is made to enter λ into the corresponding pivot row. As a consequence, one of the slack variables, let say y_k , leaves the BV and this means its counterpart plastic multiplier x_k , obtains primary permission for entering BV. In this way, there always exist a free plastic multiplier (FPM) that is ready to enter BV, but first it should be investigated what will result in the maximum gain in the objective function.

- Step 2. As a simplex rule, the variable that enters BV is the one with the most negative cost coefficient (COST_{\min}) and it can be either FPM or one of the previously expelled out slack variables.
- Step 3. If, based on the most negative cost, a slack variable is selected for entering BV, it is most likely that an unloading is taking place and more investigations are needed to make a correct decision. In such cases the algorithm is to be followed from Step 9, otherwise the algorithm continues through Step 4.
- Step 4. If FPM has the most negative cost, it means that another yield surface is becoming active. According to the simplex rules, FPM (hypothetically x_i) is to be inserted in the row j which corresponds to the smallest non-negative ratio $b_j/\overline{C}(j, i)$. Physical interpretation of such selection lies on the positiveness of plastic multiplier increments. If a row is excluded from $b_j/\overline{C}(j, i)$ -check, it may result in negative increment (decrease) of its corresponding basic variable. However for the perfect plasticity this is not the case, but in the proposed method this lemma can be utilized (by intentionally excluding the row corresponding to λ from the pivot row search) to rule out the negative load increments problems addressed in [16]. Also, if there exist more than one free row with the same smallest ratios, it mathematically means that “there might be multiple stationary points” and physically is interpreted as “possible bifurcation in the solution”, which is not the case in perfect plasticity again. It happens to have such a situation in symmetric frames which is not really a bifurcation. Fortunately such cases do not produce any problem in perfect plasticity.
- Step 5. It may happen that the selected pivot row be already occupied by another plastic multiplier. If this is the case, unloading of the obstacle plastic multiplier (OPM) is required in order to prepare conditions for entering FPM. Otherwise, solution procedure has to be followed as described in the next step.

- Step 6. If FPM belongs to a section in which one of its yield planes is already active, it means that two yield planes from a single section tend to be active simultaneously. At this stage, another restriction that is not accounted for in holonomic approaches will be considered. This case is recognized as “*staying on corner*”, and the algorithm should be followed from Step 12. Otherwise, the process is followed from Step 7.
- Step 7. If the FPM is not from an active section it can enter into BV and pivoting is made around $\overline{\mathbf{C}}(j, i)$ in order to enter FPM into selected pivot row j . Obviously this pivoting will potentially cause changes in problem variables, i.e., plastic and load multipliers, and loading process continues in this way.
- Step 8. As it was mentioned in Step 5 it happens that the selected pivot row contains some obstacle plastic multiplier (OPM) which prevents joining FPM into BV. This is a trivial case of unloading and one of the *events* introduced before. In such cases OPM is to be exited after *resetting*. Exiting a variable from BV is easily done by three pivotings in the working simplex table.
- Step 9. If COST_{\min} corresponds to a slack variable, say y_j , more verifications are needed to make a correct decision. As a consequence of complementarity, it is obvious that returning any previously expelled out slack variable y_j into BV, will be possible only if its counterpart plastic multiplier x_j (hereafter SPM) leaves BV. On the other hand and after any probable unloading, algorithm will go back to the FPM (suppose it is x_i) to enter it into BV, during which it happens that the row corresponding to the exited SPM be selected as the pivot row. If this happens, SPM will return into BV immediately after exit and the performed pivot actions impose some vain computational costs on the analysis. To avoid such situations, it is only necessary to consider the sign of some index ratio r defined as follows:

$$(3.2) \quad r = \frac{\overline{\mathbf{C}}(j, i)}{\overline{\mathbf{C}}(j, j)}.$$

In fact, the calculated index ratio r is the value that will appear in the cell (j, i) of $\overline{\mathbf{C}}$ matrix after performing required refreshments toward exiting SPM. A negative index ratio r guarantees that j row will not be selected during next pivot row search and SPM has to be expelled out. In the case of positive index ratio r , variables corresponding to the next minimums in cost row have to be verified.

- Step 10. If SPM shows immediate return tendency, the next $COST_{\min}$, i.e., 2nd, 3rd, ... minimums in the cost row should be considered. This loop is repeated until a slack variable fulfills returning criteria (as described in Step 9) or FPM obtains the most negative cost among the remaining shadow cost coefficients.
- Step 11. If $r < 0$, for sure an unloading will happen. Therefore, the process of unloading can be followed after *resetting*. It is worth noting that it is possible to have simultaneous unloading in several sections until FPM becomes qualified for entering BV. In such cases, as it is seen in the flowchart, unloadings will happen successively one after another through the loop passing Steps 2-3-9-11-2. The interesting point is that because of *resetting* there will be no changes in variable values, i.e., load and plastic multiplier increments remain zero until FPM enters.
- Step 12. If FPM is from an active critical section and qualified for entering into BV, the case is “*staying on corner*” obviously. In such cases only a re-setting is needed before entering FPM into BV.

In the case of reaching a termination criterion, i.e., maximum load, target sway/deflection, etc., the corresponding row will be selected as pivot row and after pivoting, no FPM could be found to continue the process and the algorithm stops.

Table 1. Schematic initial simplex table.

	x_1^1	x_1^2	...	x_1^m	...	x_n^1	x_n^2	...	x_n^m	λ	y_1^1	y_1^2	...	y_1^m	...	y_n^1	y_n^2	...	y_n^m	γ	δ	b	
y_1^1	*	*	...	*		*	*	...	*	*	1												1
y_1^2	*	*	...	*		*	*	...	*	*		1											1
\vdots	\vdots	\vdots	\ddots	\vdots		\vdots	\vdots	\ddots	\vdots	\vdots			\ddots										\vdots
y_1^n	*	*	...	*		*	*	...	*	*				1									1
\vdots			\ddots					\ddots															\vdots
y_n^1	*	*	...	*		*	*	...	*	*						1							1
y_n^2	*	*	...	*		*	*	...	*	*							1						1
\vdots	\vdots	\vdots	\ddots	\vdots		\vdots	\vdots	\ddots	\vdots	\vdots													\vdots
y_n^n	*	*	...	*		*	*	...	*	*												1	1
γ	*	*	...	*		*	*	...	*	*	0	0	...	0	...	0	0	...	0	1			$\bar{\lambda}$
δ	*	*	...	*		*	*	...	*	*	0	0	...	0	...	0	0	...	0	1			$\bar{\Delta}$
Cost	-1	-1	...	-1	...	-1	-1	...	-1	0	0	0	...	0	...	0	0	...	0	0	0	0	0

The proposed algorithm was explained using the standard simplex method for better understanding; however, evidently the proposed method can be consistently employed with the revised simplex method [21] to reduce computational

cost and required storage memory. In the revised simplex algorithm, only changes in $\bar{\mathbf{C}}$ are calculated and an updated form of any column of $\bar{\mathbf{C}}$ matrix is determined easily by multiplying the $\bar{\mathbf{C}}$ matrix into its original form. Furthermore, instead of calculating and storing the whole content of $\bar{\mathbf{C}}$ matrix, only its required column can be calculated and stored. Details on implementing such techniques are not discussed here for the sake of brevity.

In the proposed procedure, “exactness” and “stability” of the step-by-step approach are preserved and the deficiency of step-by-step method is fully dissolved. In other words, suitable features of both fully-holonomic, and step-by-step methods are integrated in the proposed algorithm.

4. Illustrative examples

In order to validate the proposed algorithm numerically, some examples that have been previously solved by (A) COCCHETTI and MAIER using step-by-step approach [16] and (B) TANGARAMVONG and TIN-LOI in a stepwise holonomic manner [17] are considered in the following.

A. For the frame considered in [16], pure flexural plastic hinges with no interaction between the axial force and bending moment are attributed into the critical sections. It is obvious that for this example the proposed formulation has to be modified. This is simply done by putting aside the axial force and its corresponding yield planes and variables during problem formulation. Details on such modification are not discussed here for the sake of brevity.

EXAMPLE A1. The single-bay single-story frame shown in Fig. 3 is considered as the first example with $F = 100$ kN, $H = 3$ m and $L = 4$ m. As shown, the frame is loaded with proportionally increasing lateral and gravity point loads

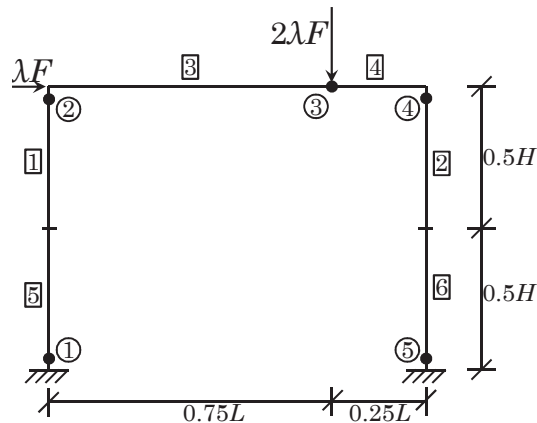


FIG. 3. Single-bay, single-story bending frame of Example A1, [16].

and the goal is to determine response of the structure and its corresponding load limit. To avoid any collapse and confine the analysis results into small deformations regime, horizontal sway of the topmost story is limited to 0.02 m. Mechanical properties of the frame members and sections are given in the Tables 2 and 3, respectively.

Table 2. Mechanical properties for the frame of Example A1.

Element	Axial stiffness (MN)	Flexural stiffness (MN · m ²)
1, 2	1953	33.99
3, 4, 5, 6	2740	79.31

Table 3. Bending capacity for the frame of Example A1.

Section	Bending capacity (kN · m)
1, 5	236.8
2, 3, 4	420.7

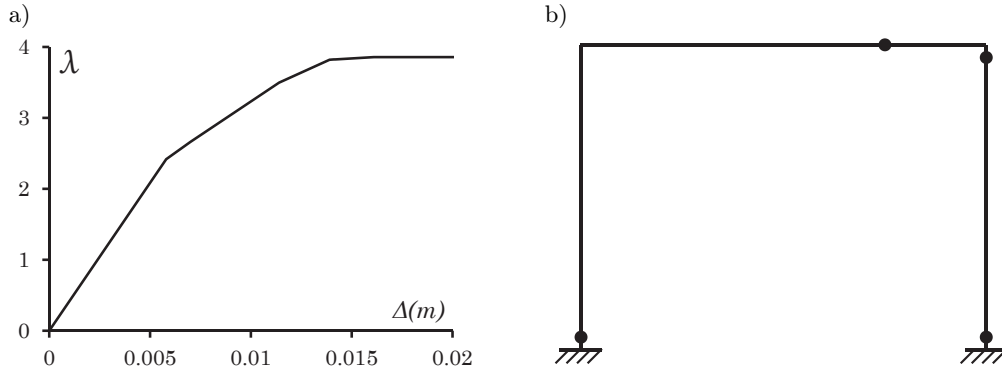


FIG. 4. Results of Example A1: a) history of story sway and b) active plastic hinges at limit load.

Formulating the problem and starting load application reveals that plasticity initiates in Section 4 at the load level $\lambda = 2.4175$. Afterwards, the sections 5, 3 and 1 will experience plasticity in sequence to turn the frame into a mechanism at the load level $\lambda = 3.8571$. The load-displacement history and plastic hinge locations at collapse load are shown in Fig. 4. The results coincide with the exact responses given in [16].

B. In this section, for all of the following examples, the material is considered to behave elastic-perfectly plastic and a simplified six-line yield surface, like that of Fig. 1 with $\bar{N}_0 = 0.15$, is adopted for its constitutive model. To pre-

vent any probable collapse, the horizontal sway at the topmost story is limited to $\bar{\Delta} = 0.75$ m. Also all frames are made from steel for which the elasticity modulus is assumed to be $E = 200$ GPa.

EXAMPLE B1. Figure 5 demonstrates the layout of a steel single-bay, three-story frame with eccentric bracings. Geometrical and mechanical properties of the frame sections are listed in Table 4.

Table 4. Member geometric and mechanical properties for the frame of Example B1.

Element	Cross section	Axial limit load (kN)	Bending limit load (kN · m)
Column	310UC118	4200	548.8
Beam	200UB18.2	742.4	57.6
Bracing	SHS125/125/9	1365	57.75

The aim of this example is to determine the exact structural responses using the proposed algorithm.

By formulating the problem and following the proposed algorithm it was observed that the first plastic hinge appears at the load level $\lambda = 57.8529$ in a beam section. At $\lambda = 67.9769$, internal force state in sections A and B (indicated in Fig. 5) reaches a corner and tends to switch the yield plane. Refreshing the formulation and continuing solution process, reveals that at load level $\lambda = 122.8044$

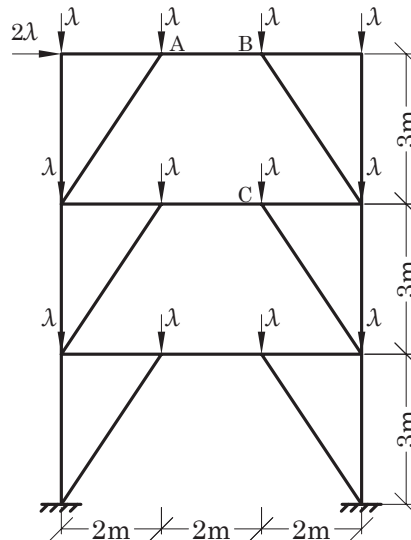


FIG. 5. Single-bay, three-story eccentrically braced frame of Example B1, [17].

internal force state in Section C tends to stay on the corner of yield loci, and, finally, at load level $\lambda = 122.9362$, the structure meets its maximum sway of 0.75 m at the topmost story and the solution terminates. Running the algorithm with a larger allowable sway, returns $\lambda = 124.1482$ as the ultimate load for this frame.

Load levels 57.853, 122.986 and 124.148 are reported in [17] as the load levels corresponding to plasticity initiation, reaching target sway and collapse load, respectively.

The exact internal forces, nodal displacements and internal plastic deformations are obtained in a straightforward manner using the proposed algorithm. The history of topmost story sway and layout of the plastic hinges, corresponding to the lateral sway 0.75 m, are shown in Fig. 6.

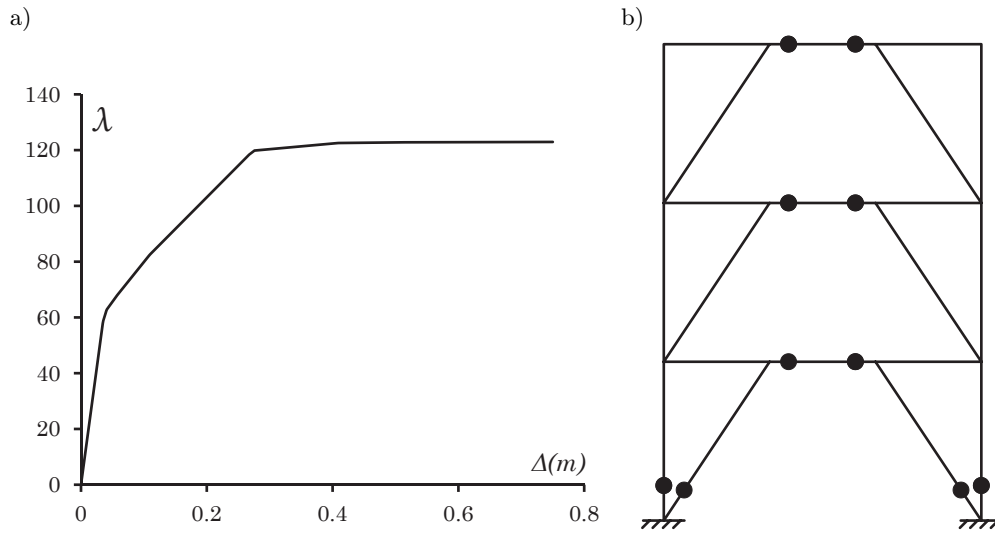


FIG. 6. a) Top story sway, b) final layout of the plastic hinges for the bending frame of Example B1.

EXAMPLE B2. Figure 7 demonstrates layout of a steel three-bay, three-story frame reinforced by the means of eccentric bracings. Geometrical and mechanical properties of the frame sections are as listed in Table 5.

Table 5. Member geometric and mechanical properties for the frame of Example B2.

Element	Cross	Axial load capacity (kN)	Bending capacity (kN · m)
Column	310UC118	4200	548.8
Beam	200UB25.7	1046.40	102.08
Bracing	150UC30	1235.20	80

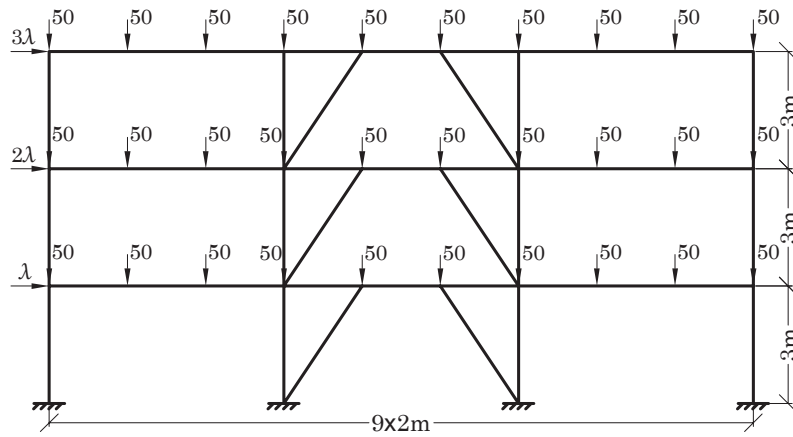


FIG. 7. Three-bay, three-story braced frame of Example B2, [17].

In this example, some constant 50 kN dead loads are applied onto the structure prior to increasing lateral forces. It is easily verified that these set of gravity loads do not cause any yield or plasticity initiation in the frame. Accordingly,

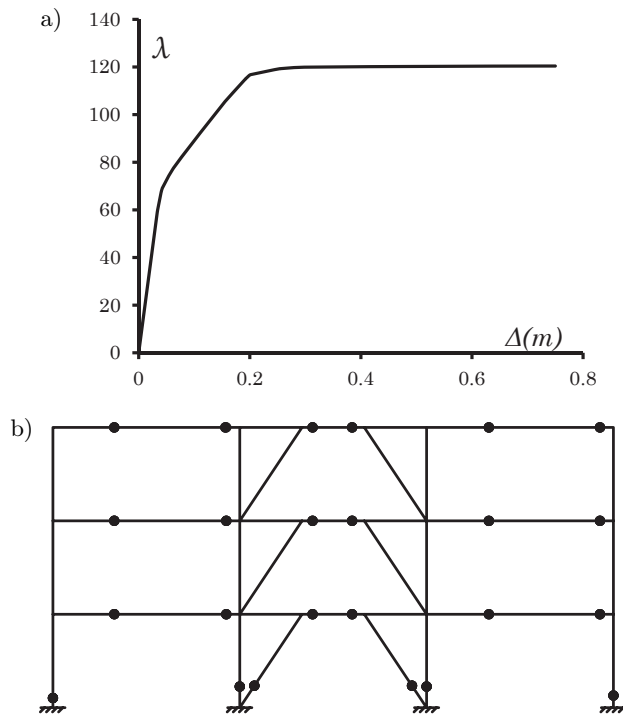


FIG. 8. a) Top story sway, b) final layout of the plastic hinges for the bending frame of Example B2.

the effects of dead loads are simply accounted for by deducing the corresponding internal forces from the initial strength capacity of frame sections. In this example, the nonlinear response of the structure is sought using the proposed algorithm.

Utilizing the proposed algorithm, it was observed that the plasticity starts at load level $\lambda = 59.0592$ in a beam section. At load level $\lambda = 82.2385$, for which frame experienced plasticity in 12 critical sections, internal force state at the ends of top story link beam reaches to yield surface corner and tends to switch the yield plane. After that, various types of events occur over the critical sections to reach target sway 0.75 m at load level $\lambda = 120.4169$.

For this frame, assigning a larger allowable sway and following the proposed algorithm, the ultimate load is determined to be $\lambda = 120.6444$. Reference [17] reports $\lambda = 59.059$ for plasticity initiation, $\lambda = 120.436$ as load level corresponding to the target sway 0.75 m and $\lambda = 120.644$ as the collapse load level.

Herein, again the exact structural responses are obtained using the proposed algorithm. History of top story sway and layout of the plastic hinges, corresponding to the lateral sway 0.75 m, are shown in Fig. 8.

EXAMPLE B3. As the last example, the multi-story bending frame of Fig. 9 is considered. The frame is subjected to proportionally increasing gravity and lateral loads. Geometrical and mechanical properties of the frame sections are as listed in Table 6. The aim of this example is to show the capability of the proposed method in solution of large scale problems.

Table 6. Member geometric and mechanical properties for the frame of Example B3.

Element	Cross section	Axial limit load (kN)	Bending limit load (kN · m)
Column	400WC328	11704	1988
Beam	460UB82.1	3150	552

In this problem, the first plastic hinge appears at the load level $\lambda = 55.3585$. At load level $\lambda = 88.8621$, where plastic hinges developed in 64 critical sections, unloading started to take place at some sections. Following the algorithm, variety of events were detected before reaching the target sway at the load level $\lambda = 91.8254$. At this stage of loading, frame experienced plasticity in 79 sections. Ignoring the sway limit and following further load application, turned out the frame ultimate load to be $\lambda = 93.7237$. For this example, [17] reports $\lambda = 55.359$ for the plasticity initiation load level, $\lambda = 91.754$ as the load level corresponding to the target sway 0.75 m and $\lambda = 93.724$ as the collapse load.

Using the proposed algorithm, the exact internal forces, nodal displacements and internal plastic deformations are obtained. The history of top story sway is

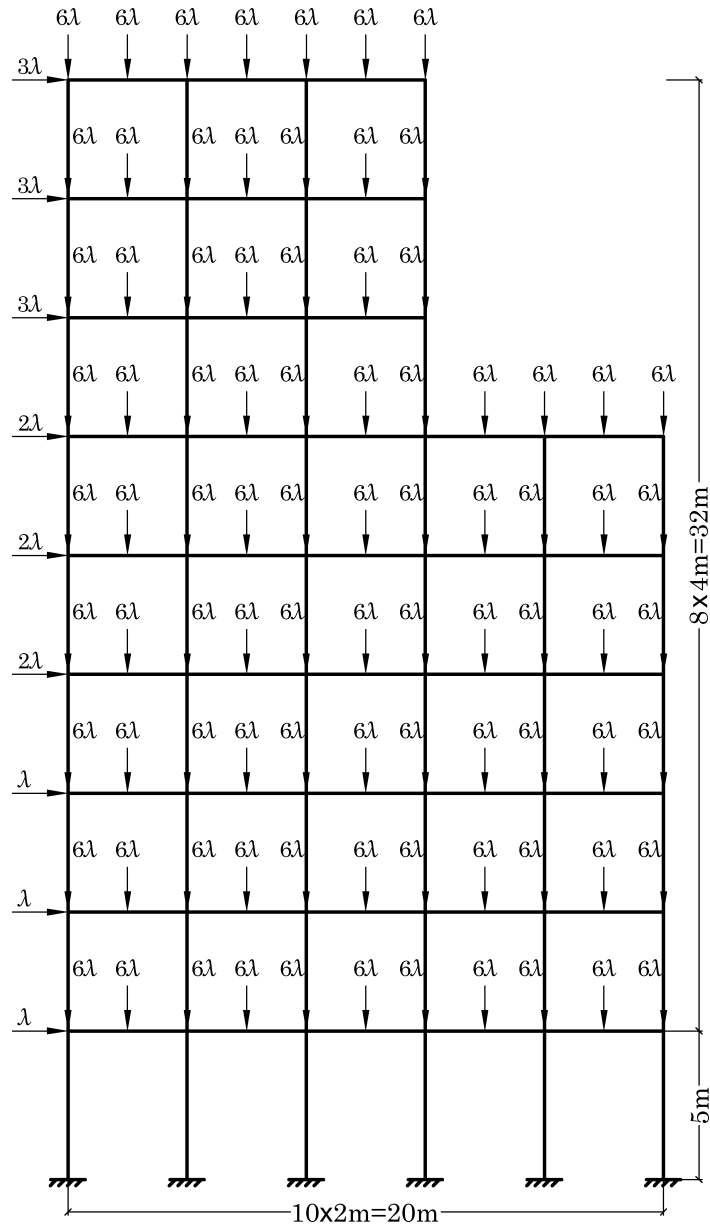


FIG. 9. Multistory bending frame of Example B3, [17].

displayed in Fig. 10a. Also the layout of active (●) and passive (○) plastic hinges, corresponding to 0.75 m sway is shown in Fig. 10b. The plastic joint disposition resulted here is slightly different from the one reported in [17] and no passive plastic joint is reported there.

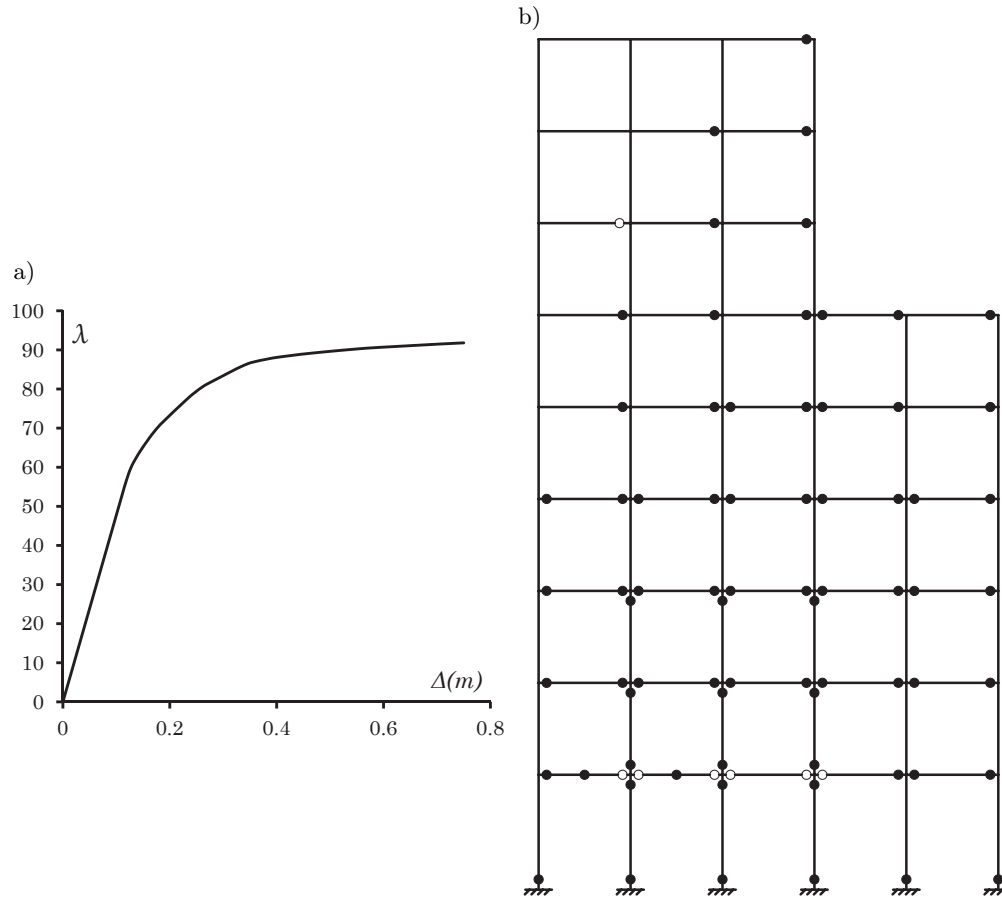


FIG. 10. Results of nonlinear analysis for the bending frame of Example B3.

5. Conclusions

Nonlinear analysis of frames composed of elastic-perfectly plastic materials were formulated and studied on the basis of mathematical programming. The solution algorithms available in literature were discussed and it was shown that those approaches could be classified into two categories: first, those accounting for path-dependency of nonlinear problems and following a step-by-step scheme and returning an exact solution, and second, those ignoring path-dependency on the whole or some intervals of loading, known as fully or stepwise holonomic. Advantages and disadvantages of each group were discussed and a new approach based on dissipated energy maximization (DEM) was proposed. The proposed approach not only holds the two distinct beneficial features of step-by-step method, namely “exactness” and “stability”, but also contains the efficiency

of holonomic approaches (without their deficiencies) by utilizing variable large steps that are determined automatically during solution process. Several examples were solved to show the capabilities and efficiency of the proposed method in finding the exact response of the structures. The major findings of DEM could be summarized as follows:

- a) The governing MP problem is easily coded for computer application. The solution algorithm is robust and reliable and unlike other methods does not require especial care for numerical instabilities and suitable load step size; neither is trapped in local extremums.
- b) Excluding round-off errors and errors due to piecewise linearization of yield surface, the proposed method is theoretically free of error and the load levels, for which a free of error solution is expected, are captured automatically.
- c) For each automatically determined load step, the CLP solution is obtained straightforward from the maximum dissipation criterion, which is believed to be the main novelty of the proposed algorithm. Although in the step-by-step method the sub-problems, that are formed and solved in each step, are small, but it is obvious that as the plasticity spreads over the frame sections, the size of the so-called “*active set*” problem becomes bigger and bigger. Accordingly, each time that a new hinge develops, a new problem has to be established and solved from the very beginning. Whereas in the proposed method, the current simplex table is easily refreshed to represent the latest status of the structure, and the solution process is continued instead of starting from the very beginning.
- d) By the aid of revised simplex method, the proposed method turns out to be very efficient even in the sense of CPU time. Using the proposed algorithm, the first three examples were solved in a fraction of a second, and the CPU time for the last one did not exceed 6.5 seconds.

The algorithm proposed herein can be used for problems with softening behavior; this will be discussed in future publications.

Appendix A

The plastic work rate \dot{W}^P is defined in terms of internal forces p and plastic deformations rate \dot{u}^P as follows:

$$(A.1) \quad \dot{W}^P = p^T \dot{u}^P.$$

Using the normality rule, Eq. (2.6), the plastic deformations rate can be replaced in terms of yield matrix Φ and the rate of plastic multipliers \dot{x} to obtain:

$$(A.2) \quad \dot{W}^P = p^T \Phi \dot{x} = (\Phi^T p)^T \dot{x}.$$

At any loading instance, the non-active critical sections can only assume zero plastic multiplier rates (as a result of the complementarity condition) and, accordingly, such sections do not contribute in the energy dissipation. On the other hand, for the active sections the (normalized) yield conditions, defined by Eq. (2.3), will hold as a set of equalities:

$$(A.3) \quad \Phi^T \mathbf{p} = \{1\}.$$

Accordingly, being the complementarity conditions satisfied (which is guaranteed in the proposed approach), the plastic work rate reads

$$(A.3) \quad \dot{W}^P = \{1\}^T \dot{\mathbf{x}}.$$

As it can be seen, the sum of plastic multipliers rates represent dissipated power as a consequence of normalizations of yield functions in perfect plasticity.

Appendix B

The linear complementarity problem (LCP), in rates once restricted only to active yield functions $\mathbf{Y}' = \mathbf{0}$ and relevant plastic multipliers \mathbf{x}' , can be written as follows:

$$(B.1) \quad \begin{cases} \dot{\lambda} = 1, \\ \dot{\mathbf{Y}}' = \dot{\lambda} \Phi'^T \mathbf{p}^0 + \Phi'^T \mathbf{p}^v \Phi' \dot{\mathbf{x}}' \leq 0, \\ \dot{\mathbf{x}}'^T \dot{\mathbf{Y}}' = 0, \\ \dot{\mathbf{x}}' \geq 0. \end{cases}$$

Being the matrix \mathbf{p}^v negative semi-definite (see, e.g., [9]), when the load amplifier λ is below the collapse value (i.e., no vector $\dot{\mathbf{x}}' \neq 0$ exists, as a solution to (B.1), implying a zero stress rate due to plastic strain rate $\dot{\mathbf{p}}^P = \mathbf{p}^v \Phi' \dot{\mathbf{x}}' = 0$), the solution to the above LCP is unique (see, e.g., [10]). Then, the same problem can be formulated in this equivalent form:

$$(B.2) \quad \max_{\dot{\mathbf{x}}'} \|\dot{\mathbf{x}}'\| \quad \begin{cases} \dot{\lambda} = 1, \\ \dot{\mathbf{Y}}' = \dot{\lambda} \Phi'^T \mathbf{p}^0 + \Phi'^T \mathbf{p}^v \Phi' \dot{\mathbf{x}}' \leq 0, \\ \dot{\mathbf{x}}'^T \dot{\mathbf{Y}}' = 0, \\ \dot{\mathbf{x}}' \geq 0, \end{cases}$$

where the objective function $\|\dot{\mathbf{x}}'\|$ is the sum of the active plastic multipliers rate.

An equivalent form of the above problem can be stated in terms of increments:

$$(B.3) \quad \max_{\Delta \mathbf{x}'} \|\Delta \mathbf{x}'\| \quad \begin{cases} \Delta \lambda = 1, \\ \Delta \mathbf{Y}' = \Delta \lambda \Phi'^T \mathbf{p}^0 + \Phi'^T \mathbf{p}^v \Phi' \Delta \mathbf{x}' \leq 0, \\ \Delta \mathbf{x}'^T \Delta \mathbf{Y}' = 0, \\ \Delta \mathbf{x}' \geq 0, \end{cases}$$

but, then, the solution has to be scaled in order to fulfill all the inactive yield functions Y'' :

$$(B.4) \quad Y'' = Y_0'' + \Delta Y'' = Y_0'' + \Delta \lambda \Phi''^T p^0 + \Phi''^T p^v \Phi' \Delta x' \leq 0.$$

So, the last set of inequalities can be directly included in the solving problem to replace the condition on the load amplifier increment $\Delta \lambda$ (note, in addition, that $Y'_0 = 0$):

$$(B.5) \quad \max_{\Delta x', \Delta \lambda} \|\Delta x'\| \left| \begin{array}{l} Y' = Y'_0 + \Delta Y' = \Delta \lambda \Phi'^T p^0 + \Phi'^T p^v \Phi' \Delta x' \leq 0, \\ Y'' = Y_0'' + \Delta Y'' \leq 0, \\ \Delta x'^T \Delta Y' = 0, \\ \Delta x' \geq 0, \end{array} \right.$$

namely:

$$(B.6) \quad \max_{\Delta x', \Delta \lambda} \|\Delta x'\| \left| \begin{array}{l} Y = Y_0 + \Delta Y = Y_0 + \Delta \lambda \Phi^T p^0 + \Phi^T p^v \Phi' \Delta x' \leq 0, \\ \Delta x'^T \Delta Y' = 0, \\ \Delta x' \geq 0. \end{array} \right.$$

The proposed modified simplex method solves this last maximization problem at each step, by implicitly accounting for the complementarity condition $\Delta x'^T \Delta Y' = 0$ and the inequality constraints.

References

1. M.A. CRISFIELD, *Non-linear Finite Element Analysis of Solids and Structures, Volume 1: Essentials*, John Wiley & Sons, Baffins Lane, Chichester, West Sussex PO19 1UD, England, 1997.
2. M.A. CRISFIELD, *Non-linear Finite Element Analysis of Solids and Structures, Volume 2: Advanced Topics*, John Wiley & Sons, Baffins Lane, Chichester, West Sussex PO19 1UD, England, 1997.
3. O.C. ZIENKIEWICZ, R.L. TAYLOR, *The Finite Element Method*, 5th ed., Butterworth-Heinemann, Oxford, 2000.
4. M. JIRASEK, Z.P. BAZANT, *Inelastic analysis of structures*, Wiley, Chichester, 2002.
5. R. HILL, *The Mathematical Theory of Plasticity*, Oxford University Press, Oxford, 1950.
6. H.J. GREENBERG, W. PRAGER, *Limit design of beams and frames*, Proceedings ASCE, **77**, 59, 1–12, 1951.
7. G. MAIER, *A quadratic programming approach for certain classes of non linear structural problems*, *Meccanica*, **3**, 2, 121–130, 1968.
8. G. MAIER, *Quadratic programming and theory of elastic-perfectly plastic structures*, *Mecanica*, **3**, 4, 265–273, 1968.

9. G. MAIER, *A matrix structural theory of piecewise-linear plasticity with interacting yield planes*, *Meccanica*, **5**, 55–66, 1970.
10. R.W. COTTLE, J.S. PANG, R.E. STONE, *The linear complementarity problem*, Academic Press, San Diego, 1992.
11. G. MAIER, S. GIACOMINI, F. PATERLINI, *Combined elastoplastic and limit analysis via restricted basis linear programming*, *Computer Methods in Applied Mechanics and Engineering*, **19**, 21–48, 1978.
12. J. HOLNICKI-SZULC, J. GIERLINSKI, *Structural modifications simulated by virtual distortions*, *Int. J. Numer. Methods Eng.*, **28**, 645–66, 1989.
13. A. GAWECKI, M.S. KUCZMA, P. KRUGER, *Analysis of slackened skeletal structures by mathematical programming*, *Computers and Structures*, **69**, 639–654, 1998.
14. G. MAIER, V. CARVELLI, G. COCCHETTI, *On direct methods for shakedown and limit analysis*, *European Journal of Mechanics A/Solids*, **19** (Special Issue), S79–S100, 2000.
15. F. GIAMBANCO, *Elastic plastic analysis by the asymptotic pivoting method*, *Computers and Structures*, **71**, 215–238, 1999.
16. G. COCCHETTI, G. MAIER, *Elastic-plastic and limit-state analyses of frames with softening plastic-hinge models by mathematical programming*, *International Journal of Solids and Structures*, **40**, 7219–7244, 2003.
17. S. TANGARAMVONG, F. TIN-LOI, *Simultaneous ultimate load and deformation analysis of strain softening frames under combined stresses*, *Engineering Structures*, **30**, 664–674, 2008.
18. G. MAIER, *Piecewise linearization of yield criteria in structural plasticity*, *Solid Mechanics Archives*, **2/3**, 239–281, 1976.
19. F. TIN-LOI, *A yield surface linearization procedure in limit analysis*, *Mechanics of Structures and Machines*, **18**, 135–149, 1990.
20. J. A. KÖNIG, *On exactness of the kinematical approach in the structural shakedown and limit analysis*, *Ingenieur-Archiv*, **52**, 421–428, 1982.
21. S.I. GASS, *Linear Programming Methods and Applications, fourth edition*, McGraw-Hill, New York, 1975.

Received June 26, 2012; revised version March 19, 2013.
